US National Oceanic and Atmospheric Administration
Climate Test Bed Joint Seminar Series
IGES/COLA, Calverton, Maryland, 24 March 2010

Summer Season Precipitation Prediction over America with the NCEP Climate Forecast System Using Different Land Components and Different Sea Surface Temperatures

Rongqian Yang, Michael Ek, Jesse Meng and Ken Mitchell

Environmental Modeling Center, NOAA/NWS/NCEP
Camp Springs, MD, 20746

1. Introduction

Skillful short-term weather forecasts, which rely heavily on quality atmospheric initial conditions, have a fundamental limit of about two weeks (Lorenz, 1963) due to the chaotic nature of the atmosphere. Useful climate forecasts on seasonal time scales, on the other hand, require well-simulated large-scale atmospheric response to slowly varying lower boundary forcings from both ocean and land surface. The critical importance of ocean memory has been well recognized (*e.g.*, Shukla, 1998; Wallace *et al.*, 1998) whereby large-scale anomalies in the atmospheric general circulation on seasonally-averaged time scales are forced first and foremost by large-scale anomalies in sea surface temperature (SST), especially over the El-Niño and Southern Oscillation (ENSO) regions of the tropical Pacific Ocean. In contrast to SST anomalies, it has been proven notably more difficult to demonstrate that land surface anomalies (soil moisture, snowpack) have meaningful positive impact on continental seasonal forecast skill in coupled climate models. Past studies show that soil moisture anomalies can persist for months (Vinnikov *et al.*, 1996), and soil moisture feedback can have notable effects on precipitation and modify other quantities through surface evaporation and surface energy processes (*e.g.*, Shukla and Mintz, 1982; Koster and Suarez, 2001; Wu and Dickinson, 2004). The feedback was also found to vary with climate regimes (*e.g.*, Koster *et al.*, 2000; Zhang *et al.*, 2008). Past studies on such land-atmosphere feedback strongly indicate that careful treatment of soil moisture and its associated anomalies in coupled climate models is important to improving seasonal predictions.

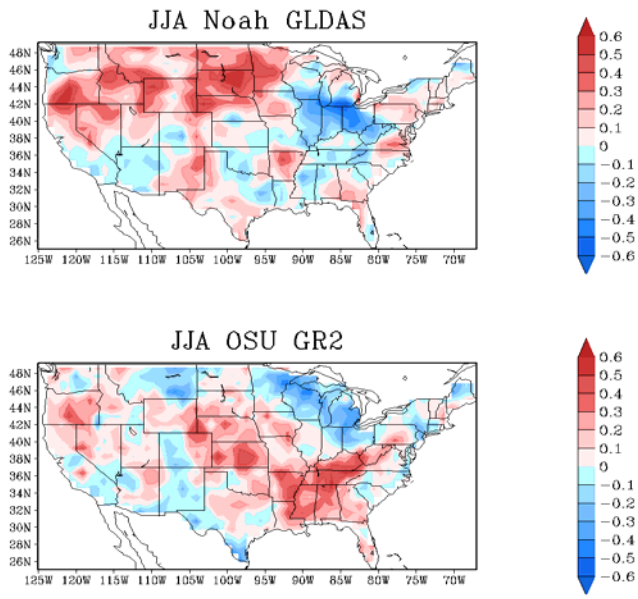

Fig. 1 Predicted JJA precipitation anomaly correlation over CONUS (25-year average).

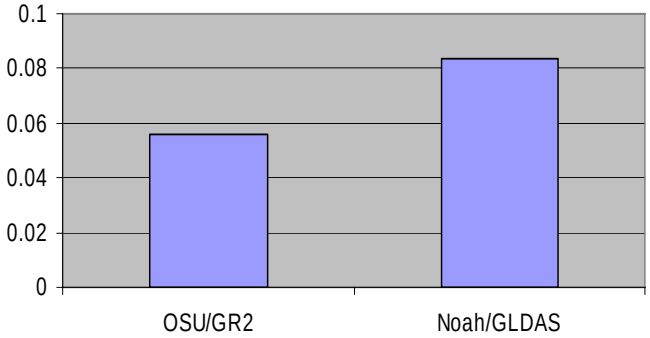

Fig. 2 CONUS-averaged predicted JJA precipitation anomaly correlation scores (25-year average).

Due to a paucity of global soil moisture observations and the complex nature of land-atmospheric interactions, land-anomaly forcing is more difficult than ocean-anomaly forcing to separate from the natural chaotic variability of seasonal circulations (*i.e.*, land-anomaly impact has a smaller signal to noise ratio than SST impact). Efforts to understand the linkage between land surface anomalies and the spawning of seasonal

Correspondence to: Rongqian Yang, Environmental Modeling Center, NOAA/NWS/NCEP, Camp Springs, MD, 20746; E-mail: Rongqian.Yang@noaa.gov

atmospheric circulation anomalies have to rely on developing more advanced land surface models. A better representation of land physics in climate models becomes the first step toward understanding how much the land contributes to climate variations. The efforts to understand the complex land-atmosphere interactions are also compounded by the fact that the prediction results from a given General Circulation Model (GCM) are sensitive to how the land-component of the GCM is initialized and the starting dates used in the integrations (*e.g.*, Dirmeyer, 2001; Koster *et al.*, 2000, 2003, and 2006). Therefore, harnessing the impact of land surface anomalies for seasonal predictions, especially over the N.H. summer season when the SST signal is weaker than in winter, is a promising challenge that requires not only a large number of members in the ensemble set of seasonal predictions (*e.g.*, Tribbia and Baumhefner, 1998; Brankovic *et al.*, 1994), but also special care in the treatment of land surface initial conditions (*e.g.*, initial soil moisture). The treatment becomes increasingly important at higher latitudes, such as the Contiguous U.S. (CONUS) where the soil moisture feedback was found to account for more variance of monthly precipitation anomalies (Zhang *et al.*, 2008). The study by Koster *et al.* (2004) also suggested that a proper global initialization of soil moisture may enhance precipitation prediction skill during the Northern Hemisphere summer season.

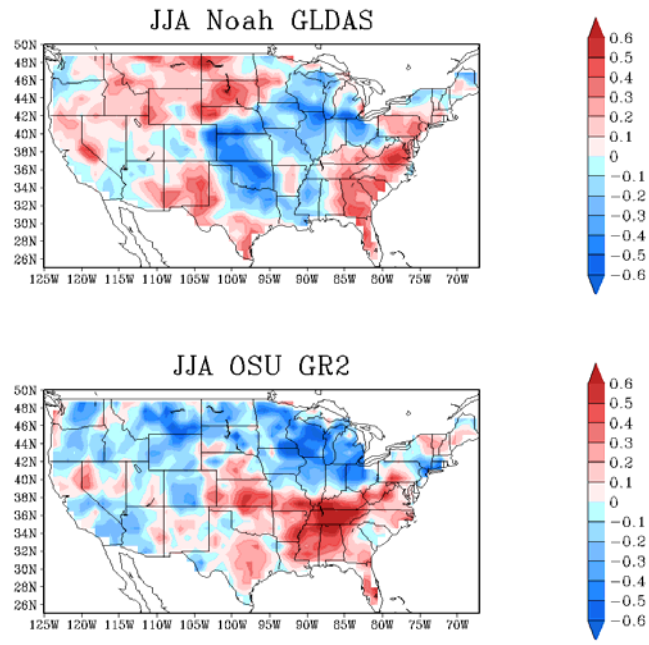

Fig. 3 Predicted JJA precipitation anomaly correlation over CONUS averaged over the 15 neutral years.

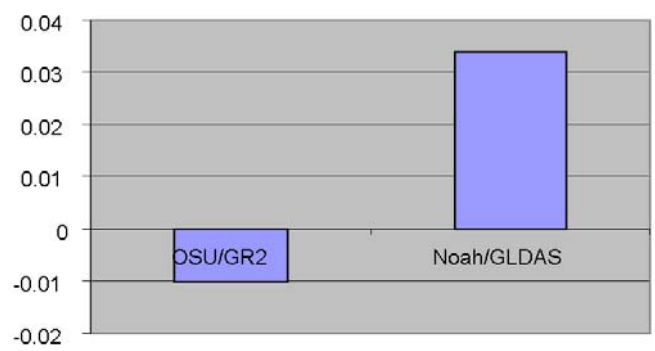

Fig. 4 CONUS-averaged predicted JJA precipitation anomaly correlation scores averaged over the 15 neutral years.

2. CFS Experiments

The next generation of NCEP Climate Forecast System (CFS) will include many advances in atmosphere, land, and ocean physics, among which the old land component (OSU/GR2 combination) used in the currently operational CFS, will be replaced with a new land component (Noah/GLDAS combination), wherein the upgrade from the OSU LSM to the Noah LSM is for inclusion of recent advances in land physics and the replacement of the old GR2 land states with the GLDAS land states is to take special care of land initializations. This study, from the land perspective, used a highly controlled approach (same atmospheric and oceanic physics, same atmospheric and oceanic initial states, same resolution, and same initial integration dates) to examine the extent to which the land upgrades (OSU to Noah LSM and GR2 to GLDAS land data assimilation system) can improve CFS summer season predictions. Experiments were first carried out over a 25-year period (1980-2004) with 10 ensemble members whose initial conditions are from mid-April to early May in fully coupled (CMIP) mode, where the old OSU LSM was initialized using the GR2 land states (CMIP OSU/GR2) and the new Noah LSM was initialized with the GLDAS land states (CMIP Noah/GLDAS). Secondly, to separate out the ocean impact, parallel experiments with both land components were also executed over the same period in an AMIP mode (*i.e.*, AMIP Noah/GLDAS and AMIP OSU/GR2), where the coupled SST was replaced by observed SST. These experiments consist of four CFS configurations. There are CMIP Noah/GLDAS, CMIP OSU/GR2, AMIP Noah/GLDAS, and AMIP OSU/GR2 respectively. Comparisons were assessed on an ensemble basis and at seasonal timescales (June-July-August: JJA). The main variable we examined is precipitation with focus over the CONUS. The main measure of CFS skill is the Anomaly Correlation (AC;

skill map), which is defined as correlation between the CFS predicted anomaly (with respect to its corresponding climatology) and the corresponding observed anomaly, where we can examine geographical patterns of the AC score, and the Area-averaged Anomaly Correlation (AAC; the bar chart), which is a single value derived from averaging the AC scores over the CONUS, where we can assess the CFS overall performance.

In addition to the evaluation of CFS skill over the entire 25 years, to provide insight into the difference in CFS performance with different SST signals, the 25 years are stratified into ENSO non-neutral and neutral years 3using the observed May-June-July (MJJ) Niño 3.4 SST anomaly magnitude of 0.7 ˚C as a threshold for non-neutral years (slightly lager than the commonly used 0.5˚C threshold, to better separate out ocean impact). As a result, the 25 years are split into 10 non-neutral and 15 neutral years. The non-neutral years are 1982, 1983, 1987, 1988, 1991, 1992, 1993, 1997, 1999, and 2002 (among which, only 1988 and 1999 are cold ENSO years and the rest are warm ENSO years) and the neutral years are 1980, 1981, 1984, 1985, 1986, 1989, 1990, 1994, 1995, 1996, 1998, 2000, 2001, 2003 and 2004, respectively. The CFS prediction skill with and without the land upgrades in both CMIP and AMIP modes is also assessed for the ENSO-neutral years to examine how much land-atmospheric interactions contribute to seasonal predictability.

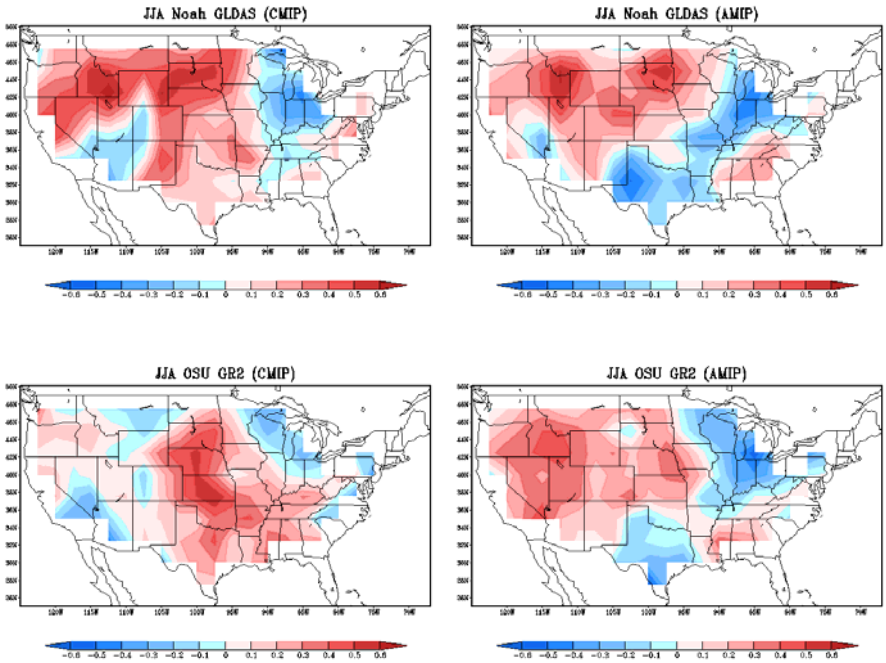

Fig. 5 JJA precipitation anomaly correlation over CONUS with CMIP (left column) and AMIP (right column) prediction modes (The left column is the same as in Figure 1, but at 2.5x2.5 degree resolution).

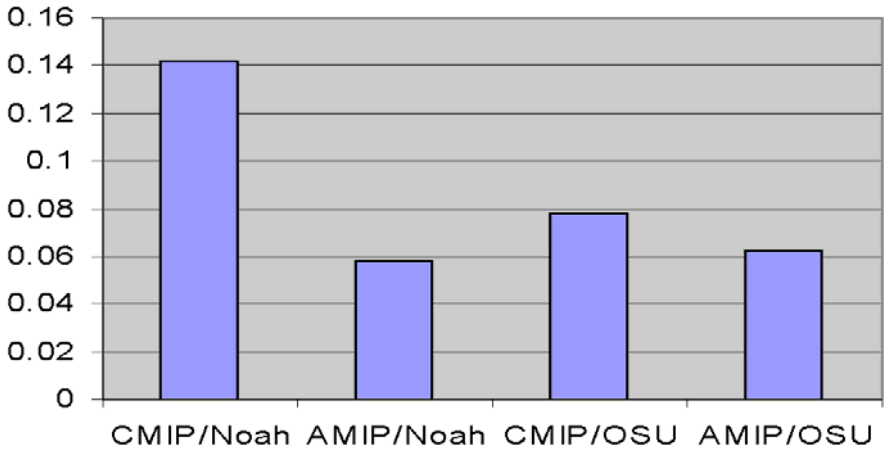

Fig. 6 CONUS-averaged JJA precipitation anomaly correlation scores with CMIP and AMIP prediction modes.

3. Main Results

Figure1 presents the CONUS AC skill map of JJA ensemble mean total precipitation over the 25-yr reforecasts from the two CMIP CFS configurations. Checking on the CFS performance over different geographical regions, Figure 1 shows that compared to the OSU/GR2 CFS, the Noah/GLDAS CFS has a larger area of high anomaly correlation scores over a majority of the western CONUS and each configuration yields different preferred regions toward better performance where the Noah/GLDAS CFS shows a tendency

toward high scores in a majority of the Pacific Northwest and the northern Great Plains, whereas the OSU/GR2 CFS appears to yield somewhat better AC scores in the southwest monsoon region and the states that border the Gulf of Mexico. Using a different measure, the bar chart of AAC in Figure 2 clearly shows that the CFS with the new component of GLDAS/Noah yields a higher value, indicating that upgrading of the OSU/GR2 combination to the Noah/GLDAS combination does improve the overall CONUS precipitation prediction. Despite this improvement with the land component upgrade over the entire 25 years, the student's t-test indicates that the difference is not statistically significant at 90% confidence level. Looking into the CFS performance over the 15 neutral years when the land-anomaly forcing has more controls over seasonal precipitation prediction, Figures 3 and 4 are as in Figures 1 and 2 but for the 15 neutral years. Figure 3 shows that the CFS precipitation prediction skill drops dramatically with both land components when the ENSO signals are weak and the degradations mainly occur over most of the relatively drier Midwest region and the Pacific Northwest states However, the Noah/GLADS CFS maintains relatively good performance over the above regions (albeit with degradation too). As shown in Figure 4, the CONUS-averaged AC scores with both configurations are much lower than their 25-year averages, where the Noah/GLDAS CFS shows a small positive value and the OSU/GR2 CFS yields a negative number. While the values are low, the student's t-test indicates that difference is significant at 90% confidence level (the Noah/GLDAS CFS is significantly better in CMIP mode during the 15 ENSO-neutral years).

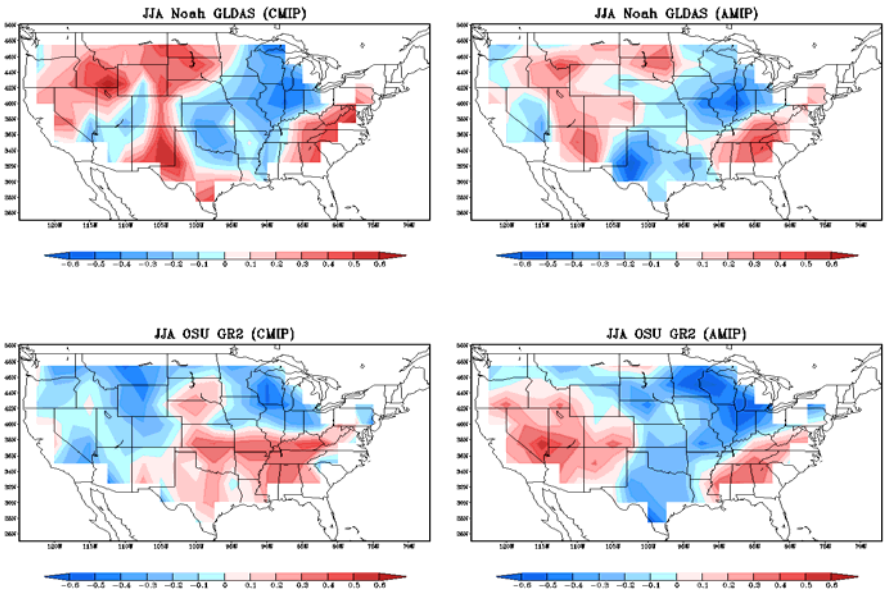

Fig. 7 JJA precipitation anomaly correlation averaged over the 15 neutral years with CMIP (left column) and AMIP (right column) modes (The left column is the same as in Figure 3, but at 2.5x2.5 degree resolution).

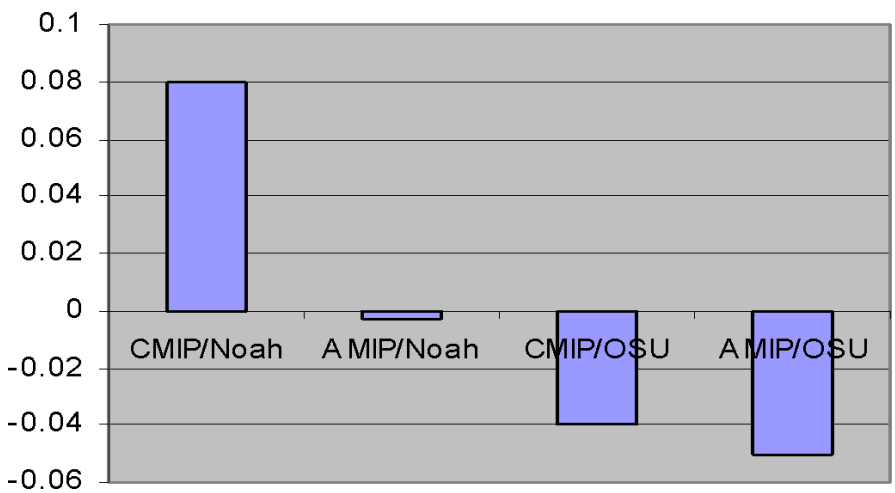

Fig. 8 CONUS-averaged JJA precipitation anomaly correlation scores averaged over the 15 neutral years with CMIP and AMIP prediction modes.

To confirm the improvement over precipitation skill is really benefited from the land upgrades and to separate out the ocean effect, an AMIP-style run was performed with both CFS configurations, where the coupled SST is replaced by the observed SST for the same 25 years. Checking on how well the CFS performs in the AMIP mode, Figure 5 presents the CONUS AC skill maps and comparison with their corresponding

coupled runs (the left column is the same as in Figure 1, but evaluated at 2.5x2.5 degree resolution to accommodate later cross-correlation analysis where the atmospheric verification data from GR2 is used. Same applies to Figure 7 below and previous Figure 3). In Figure 5, the geographic patterns of the AC skill maps with and without the land upgrades (right column) look extremely similar in the AMIP-style runs, where both CFS configurations show negative AC scores over the Midwest regions and the southern Great Plains and positive scores from the central Great Plains all the way to the Pacific Northwest. The difference lies in the magnitudes of the positive and negative values. Overall, as shown in Figure 6, the difference between the second and the fourth bar is very small and is not statistically significant at 90% confidence level. Compared to their corresponding coupled runs, the CMIP Noah/GLDAS CFS has much better performance over the southern Great Plains than the AMIP Noah/GLDAS CFS, and the CMIP OSU/GR2 CFS, except slightly degraded performance over the Pacific Northwest and the Rocky Mountains, performs better than the AMIP OSU/GR2 CFS everywhere else. On average, as also shown in Figure 6, the first bar is higher than the second bar, so is the third bar than the fourth bar. Checking on the CFS performance in AMIP mode with and without the land upgrades during the ENSO-neutral years, Figure 7 is as in Figure 5 but for the 15 neutral years. Similar to what seen in the coupled runs, the CFS skill decreases dramatically with both configurations when SST impact is weak. Both the AMIP Noah/GLDAS and the AMIP OSU/GR2 CFS have larger areas of negative AC scores than their 25-year averages. As reflected in Figure 8, the CONUS-averaged AC scores in both AMIP Noah/GLDAS (the second bar) and the AMIP OSU/GR2 CFS (the fourth bar) are negative. The difference is that the negative value is smaller with the AMIP Noah/GLDAS CFS. However, even the difference between the two negative values is small, the t-statistical test indicates that it is significant at 90% confidence level (Noah/GLDAS is significantly better than OSU/GR2 in AMIP mode during the ENSO-neutral years).

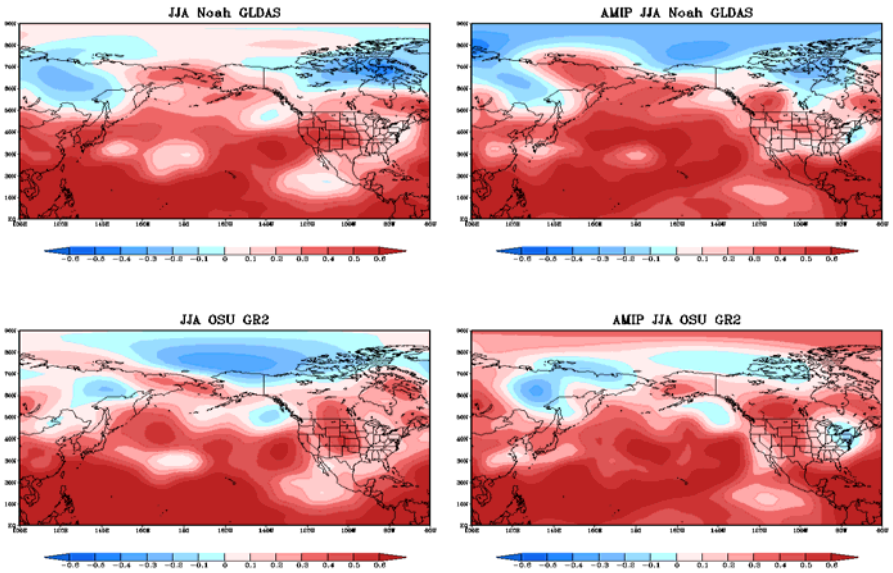

Fig. 9 JJA 500 mb GPH anomaly correlation with CMIP (left column) and AMIP (right column) prediction modes.

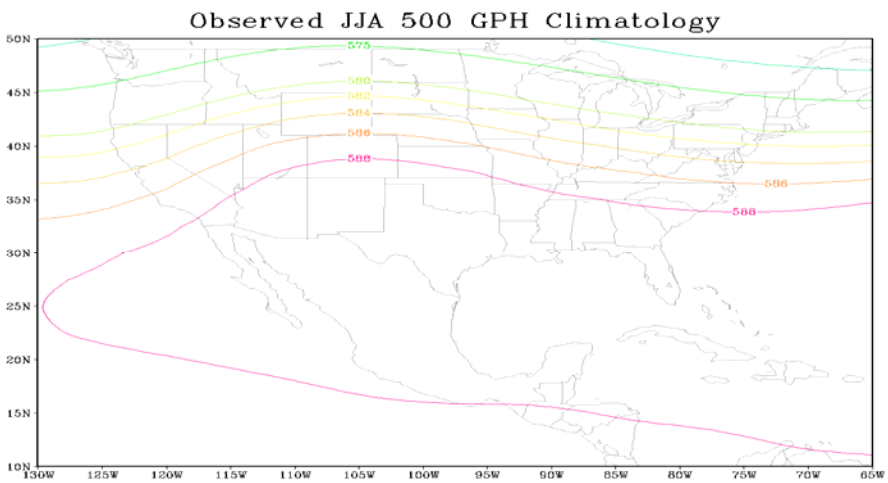

Fig. 10 JJA 500 mb GPH climatology in GR2.

To get insight into the why the AMIP-style runs are not as good as the CMIP-style runs, we examined how the land-atmosphere-ocean interactions differ with the two modes. Ocean, atmosphere and land are represented by SST, 500mb Geo-Potential Height (GPH), and soil moisture respectively. We first checked on

how SST impacts the large-scale atmospheric circulation performance in the four CFS configurations. Figure 9 presents the JJA 500mb GPH AC skill maps averaged over the 25 years. In Figure 9, the CFS in AMIP mode with both land components does a better job over most of the Pacific Ocean due to strong SST effect, but performs worse over the CONUS, especially over the Atlantic and the Gulf states than their corresponding CMIP-style runs. Looking into how well that the four CFS configurations perform in predicting JJA 500mb GPH climatology, Figure 10 presents the observed JJA 500mb GPH climatology where the extent of 588 GPH line can expand from the Four Corner states much further to the southern Mexico and the center is located over the southern Texas, which looks similar to the predicted climatology in the CMIP-style runs in Figure 11 (left column) although it's still a little bit low and the area is smaller. This is different from the climatology predicted from the AMIP-style runs (right column) where the extent of 588 GPH line is much smaller than both observation and the CMIP runs and its center is located over the state of New Mexico. This shifted center in 500mb GPH climatology causes changes in airflow patterns over the Gulf States which contribute to the skill loss as shown in Figures 5 and 7.

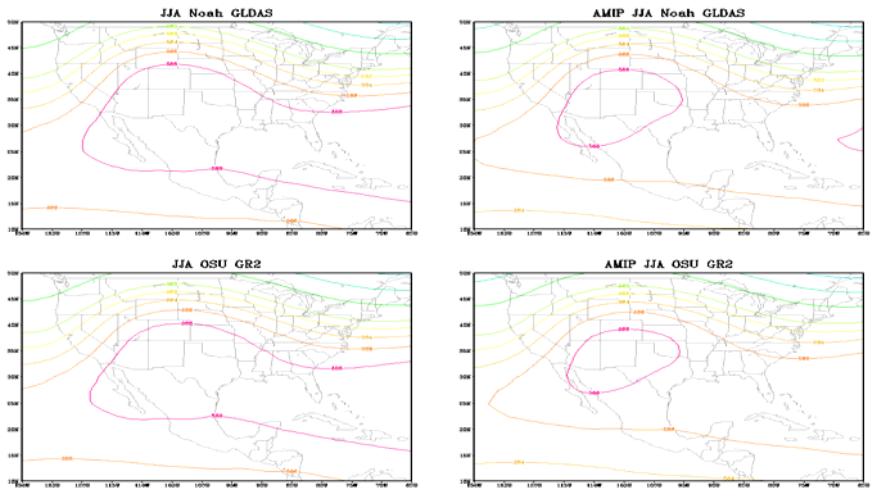

Fig. 11 Predicted JJA 500 mb GPH climatology with CMIP (left column) and AMIP (right column) modes.

Looking into how 500GPH anomaly interacts with soil moisture anomaly, Figure 12 presents their JJA anomaly cross correlations in both Noah/GLDAS and OSU/GR2 data assimilation systems. The two panels of Figure 12 show that they are all negatively correlated. The difference lies in that it is stronger in the Noah/GLDAS system. Checking on how well the CFS predicts the cross correlation in both CMIP and AMIP modes, Figure 13 shows that in the CMIP-style runs, the cross correlation with and without land upgrades has very good agreements with the observations (negatively correlated). However in the AMIP-style runs, the CFS with both land components predicts the wrong sign (positively correlated) over the Gulf and the Atlantic states. They are exactly the regions where the low JJA 500mb GPH AC skill and shifted JJA 500mb GPH climatology are located. The persistent forcing from using observed SST does not allow any feedbacks from the atmosphere and leads to changes in large-scale atmospheric circulations.

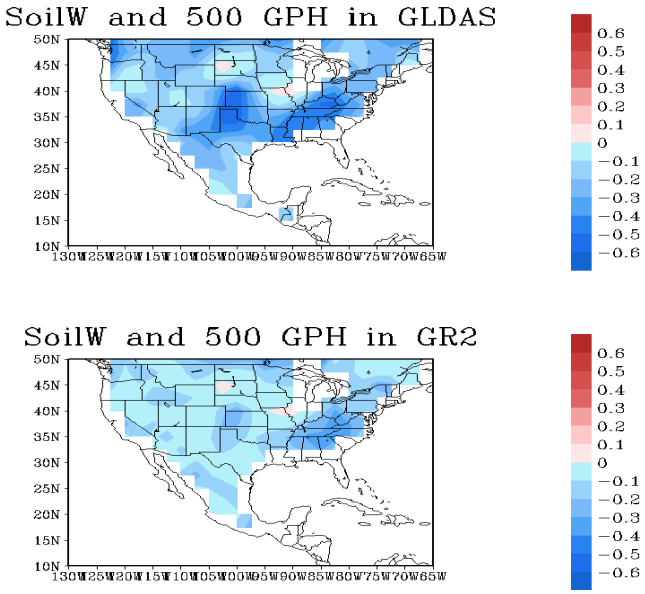

Fig. 12 JJA soil moisture and 500mb GPH anomaly cross correlation in GLDAS (top) and GR2 (bottom).

4. Conclusions

Coupled CFS experiments indicate that the land component upgrade from OSU/GR2 to Noah/GLDAS does improve the overall summer season precipitation predictions, especially during the ENSO-neutral years. Compared to the coupled runs, the CFS loses skill in the AMIP mode with both land components, but the difference is still

significant during the ENSO-neutral years, demonstrating that the improvement is really benefited from the land upgrades and more represented in the coupled mode. Ignoring any feedbacks from the atmosphere using prescribed oceanic boundary conditions will adversely affect land-atmospheric interactions, and thus degrade the CFS performance.

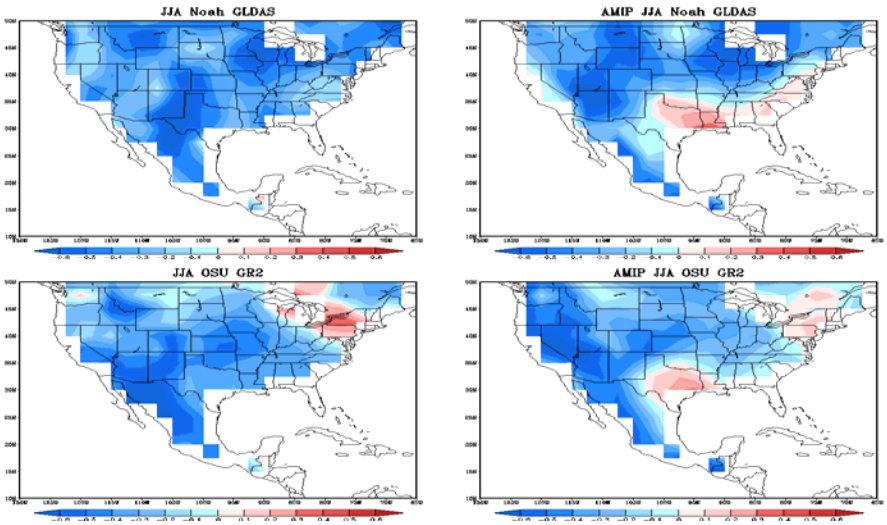

Fig. 13 Predicted JJA soil moisture and 500mb GPH anomaly cross correlation with CMIP (left column) and AMIP (right column) modes.

References

Brankovic, C., T.N. Palmer, and L. Ferranti, 1994: Predictability of seasonal atmospheric variations. *J. Climate*, **7**, 217-237.

Dirmeyer, P.A, 2001: An evaluation of the strength of land-atmosphere coupling. *J. Hydrometeorol.*, **4**, 329-344.

Lorenz, E.N., 1963: Deterministic nonperiodic flow. *J. Atmos. Sci*, **20**, 131-141.

Koster, R.D., M.J. Suarez, and M. Heiser, 2000: Variance and predictability of precipitation at seasonal-to-interannual timescales. *J. Hydrometeorol.*, **1**, 26-46.

Koster, R.D., and M.J. Suarez, 2001: Soil moisture memory in climate models. *J. Hydrometeorol.*, **2**, 558-570.

Koster, R.D., M.J. Suarez, R.W.Higgins, and H.M. Van den Dool, 2003: Observational evidence that soil moisture variations affect precipitation. *Geophys. Res. Lett.*, **30(5)**, 1241.

Koster, R.D., and Coauthors, 2004: Realistic initialization of land surface states: Impacts on subseasonal forecast skill. *J. Hydrometeorol.*, **5**, 1049-1063.

Koster, R.D., and Coauthors, 2006: GLACE: The Global Land-Atmosphere Coupling Experiment: Part 1: Overview, *J. Hydrometeorol.*, **7**, 590-610.

Shukla, J., 1998, Predictability in the midst of chaos: A scientific basis for climate forecasting. *Science*, **215**, 1498-1501.

Shukla, J., and Y. Mintz, 1982: Influence of land-surface evapotranspiration on the Earth's climate. *Science*, **282**, 728-71.

Tribbia, J. J., and D.P. Baumhefner, 1998: Estimates of the predictability of low-Frequency variability with a spectral general circulation model, *J. Atmos. Sci.*, **45**, 2306-2317.

Vinnikov, K.Y., A. Robock, N. A. Speranskaya, and C.A. Schlosser, 1996: Scales of temporal and spatial variability of midlatitude soil moisture. *J. Geophys. Res.*, **101**, 7163-7174.

Wallace, J. M., and Coauthors, 1998: On the structure and evolution of ENSO-related climate variability in the tropical Pacific: Lessons from TOGA. *J. Geophys. Res.*, **103**, 14241–14259.

Wu, W., and R.E. Dickinson, 2004: Time scales of layered soil moisture memory in the context of land-atmosphere interactions. *J. Climate*, **17**, 2752-2764.

Zhang, J., W. Wang, and J. Wei, 2008: Assessing land-atmosphere coupling using soil moisture from the Global Land Data Assimilation System and observational precipitation. *J. Geophys. Res.*, **113**, D17119, doi:10.1029/2008JD009807.